INTERNATIONAL JOURNAL OF NOVEL MATERIALS
Vol. 1, No. 2, July-December 2010, pp. 39-43

Auxeticity in Single Layer Graphene Sheets

F. Scarpa[*], S. Adhikari[**] and A. Srikantha Phani[***]

Abstract: *In this work we identify boundary conditions and types of loading for single layer graphene sheets (SLGS) suggesting an auxetic behaviour for the C-C bonds and the graphene layers. The mechanical properties of the SLGS are identified using an equivalent atomistic-continuum model proposed in [1], and compared with existing data in open literature. Under clamped-free uniaxial loading, the overall mechanical properties of the SLGS can be explained assuming an equivalent mechanical auxetic behaviour of the C-C bonds. When the SLGS have full blocked boundary conditions and undergo resonance, the minimisation of the Hamiltonian leads to the identification of equivalent negative Poisson's ratio (NPR) in the graphene sheets.*

Keywords: *Graphene, Mechanical properties, Vibration, NPR.*

1. INTRODUCTION

The discovery of an efficient method to exfoliate single layer graphene sheets (SLGS) [2] has opened a possible vast landscape of possibilities to use grapheme layers and platelets for innovative nanocomposites [3] and NEMS as mass and strain sensors [4]. The engineering of novel nanostructures based on SLGS needs however modelling techniques to represent the overall mechanical properties of the nanomaterial. The initial models proposed in open literature where based on interactions provided by axial and rotational springs on an hexagonal lattice [5]. MD and models based on Tersoff-Brenner potentials [6], as well as Cauchy-Born rule [7] have been proposed, and their results mainly benchmarked against available data from simulations, or bulk graphite properties. Only recently, experimental data on the out-of-plane properties of graphene have been made available on multilayer [8] and single layer sheets loaded with AFM tips [9]. The mechanical properties derived with the different methods published so far provide a broad agreement of the tensile rigidity between of SLGS between 0.190 and 0.350 TPa nm, according to the size and loading conditions of the graphene samples. A significant scattering is however observed for the thickness values of the graphene, a similar condition observed in single wall carbon nanotubes (the "Yakobson's Paradox" [10]). To solve the problem, a consistent number of models simply assumes the thickness of the SLGS (and carbon nanotubes) being equal to 0.34 nm, the interlayer graphite atoms distance. There is a subtle but important distinction between the pure geometric definition of thickness, and its representation in continuum mechanics. We use the concept of thickness when we intend to adopt an equivalent continuum model to represent the mechanical behaviour of the nanocomponent. In single layer graphene sheets, like in single wall carbon nanotubes, the thickness of the equivalent continuum (say a plate or an hollow tube) should be equal to the one of the C-C bonds composing the nanostructures. However, there is no physical thickness per se for the covalent bonds, nor for the carbon atoms involved. However, when the nanostructure is subjected to a mechanical static loading, it tends to reach its equilibrium state corresponding to the minimum potential energy, or the minimum of the Hamiltonian (equivalent to the total energy of the system [11]), when the loading is dynamic. The geometric and material configuration of the equivalent continuum mechanics structures (plate and/or hollow tube) will be therefore defined by the energy equilibrium conditions of the nanostructure, and cannot be ascribed as fixed. The Authors have recently formulated a modelling approach, where the equivalent homogenised properties of the graphene sheets are formulated in terms of the thickness, equilibrium lengths and force models used to represent the C-C bonds of the graphene lattice [1]. The covalent bonds are represented as structural beams with stretching, bending, torsional and deep shear deformation, based on the equivalence between the harmonic potential expressed in terms of AMBER [12] or Morse models [13], and the mechanical strain energies associated to affine deformation mechanisms. The overall mechanical properties and geometric configurations of the graphene sheets and carbon

[*] Advanced Composites Centre for Innovation and Science, University of Bristol, BS8 1TR, Bristol, UK., *E-mail: scarpa.fabrizio@gmail.com*
[**] School of Engineering, Swansea University, Singleton Park, Swansea SA2 8PP, UK.
[***] Department of Mechanical Engineering, The University of British Columbia, Vancouver, BC, V6T 1Z4, Canada.

nanotubes are then calculated minimising the total potential energy associated to models of nanostructures subjected to mechanical loading. The models are developed using finite element approaches, either representing the nanostructures as truss assemblies with the C-C bond equivalent beams, or previously homogenised mechanical properties, always in function of the force models, thickness and equilibrium length of the bonds. In this work we highlight the possible presence of negative Poisson's ratio (NPR) behaviour in single layer graphene sheets under mechanical and dynamic loading.

The Authors have already identified a significant auxeticity in the equivalent mechanical behaviour of the C-C bonds in SLGS when subjected to pure shear loading [1]. Single graphene sheets truss structures have been fully clamped at one end and loaded at the opposite side with a constant strain, and the equivalent mechanical properties (Young's modulus and Poisson's ratio v_{yx}) computed, after the minimisation of the total potential energy. The equivalent Poisson's ratio of the C-C bonds is negative, while the thickness of the graphene layer and the in-plane tensile rigidity agrees well not only with other MD-based simulations, but also the experimental values measured on circular graphene sheets under central point loading. Under resonance conditions, the minimisation of the Hamiltonian for the first and second natural frequency of a fully clamped SLGS shows not only an auxetic behaviour for the C-C bonds, but also a marginally auxetic behaviour for the whole graphene sheet, especially when considering the Morse potential as reference force model for the covalent bonds.

2. SIMULATIONS

The mechanical properties of the SLGS have been calculated from uniaxial loading performed on truss assemblies of C-C bonds represented by structural beams

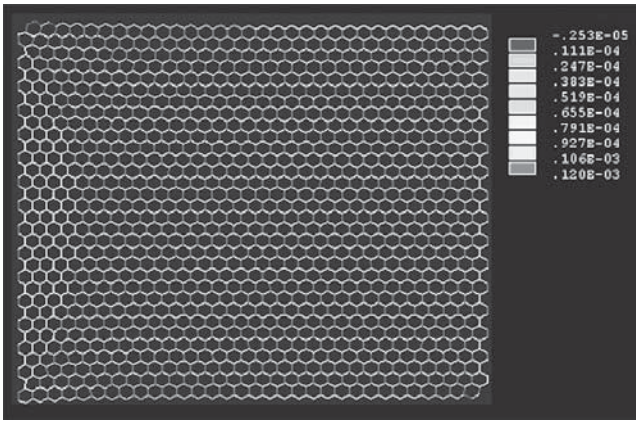

Figure 1: Axial Strains Distribution for SLGS Under Uniaxial Static Loading (*x*-Direction). Dimensions 7.16 nm × 6.55 nm.

(Fig. 1). Following [1], the equivalent mechanical properties of the beams (Young's modulus E and shear modulus G) are a nonlinear function of the type:

$$Y = Y(d, L, k_s, k_\tau, k_\theta) \tag{1}$$

where d and L are the thickness of the bond and its equilibrium length respectively, and k_s, k_τ, k_θ are the stretching, torsional and out-of-plane rotational spring constants, provided in our case by the AMBER and linearised Morse potential [1]. The equivalent beams were represented as single Finite Element Timoshenko 3D circular beams with axial, torsional and bending stiffness capabilities, and cross-section shear deformation given by the shear correction factor Ψ:

$$\Psi = \frac{6v^2 + 12v + 6}{7v^2 + 12v + 4} \tag{2}$$

where v is the Poisson's ratio of the equivalent material for the C-C bond. Eq. 2 is the exact shear correction factor for circular beams as indicated by Timoshenko [14]. The truss assemblies were subjected to the specific boundary conditions for the loading cases. For each simulation, the total potential energy or the Hamiltonian were minimised using a two-stage nonlinear optimisation simplex technique, using a zero order method to identify clusters of solutions with local minima, and a first order derivative-based method to search for the global minima of the function.

2.1 Uniaxial Tensile Loading

Three sets of SLGS with base length of 7.16 nm and varying side length (from 2.09 nm to 6.55 nm) were fully clamped on one side, and loaded at the opposite with an imposed displacement corresponding to 0.01% of uniaxial strain. Local stiffening was ensured blocking the in-plane rotational degrees of freedom of the nodes where the displacements were imposed. The linear geometric loading problem was solved using a Jacobi front wave scheme.

2.2 Resonance Conditions

Neglecting damping effects, the Hamiltonian for the SLGS can be written as [11]:

$$H = T + U \tag{3}$$

where T and U are respectively the kinetic and potential energy of the system. When the system is close to the i^{th} natural frequency, the Hamiltonian can be rewritten in terms of the i^{th} the normal mode as:

$$H_i = \frac{1}{2}\{\Phi\}_i^T [M]\{\Phi\}_i + \frac{1}{2}\{\Phi\}_i^T [K]\{\Phi\}_i \tag{4}$$

where [*K*] and [*M*] are the stiffness and mass matrix of the system respectively. Using a mass orthonormalisation for the modes [15], the Hamiltonian H_i can be rewritten as:

$$H_i = \omega_i^2 \tag{5}$$

where ω_i is the i^{th} natural frequency of the system. It must be noticed that the assumption of negligible damping is valid only when the dissipation is occurring attachment and thermoelastic losses in a typical substrate-resonator layout, for which the index Q^{-1} is of the order of $10^{-6 \div -22}$ [16].

3. RESULTS AND DISCUSSIONS

3.1 Uniaxial Tensile Loading

Table 1 shows the mechanical properties for the SLGS loaded uniaxially, with different dimensions and force models adopted. For all the dimensions of the graphene sheets, the equivalent ν of the C-C bond is strongly negative, equal to −0.78 for the AMBER model, and −0.70 for the linearised Morse potential case. The equilibrium length of the bonds is towards the minimum value in the range present in open literature. The average thickness for all the force models is around 0.056 nm, close to the 0.058 nm identified by Duan and Wang [17] in circular graphene sheets represented by the COMPASS force model, and 0.057 nm found in [18]. The Young's modulus for the AMBER case varies between 4.13 TPa and 4.38 TPa, similar to the 4.23 TPa identified by Huang *et al*., [18] using second generation Tersoff-Brenner potentials [18]. The use of the linearised Morse potential leads to an increase of the in-plane stiffness of the SLGS, with Young's modulus varying between 5.88 TPa and 6.24 TPa. Duan and Wang [17] again identify a Young's modulus of 6.10 TPa with the COMPASS force model adopted. A quantity that provides a more general comparison between the different results in open literature is the tensile rigidity Y , defined as the product between the Young's modulus and thickness of the graphene. The AMBER force model provides values of the tensile rigidity compatible with the 0.277 TPa nm of Caillerie *et al*., [19], 0.218 TPa nm of Brenner [6], and 0.243 TPa nm of Huang *et al*., [18]. On the other hand, the use of the Morse potential leads to tensile rigidities varying between 0.327 and 0.347 TPa nm, in line with the results from Tu and Ou-Yang [20] (0.348 TPa nm) and Kudin *et al*., [21] (0.345 TPa nm). The experimental values of the tensile rigidities measured by Lee *et al*., [9], and Blaklee *et al*., [22] are 0.335 TPa nm and 0.342 TPa nm respectively. The Poisson's ratio of the graphene sheet obtained loading along the *x*-direction (ν_{yx}) is higher compared to the values in open literature, which range from 0.16 [23] to 0.34 [20], with the exception of Brenner [6] (0.41). Reddy and co-Authors [7] have been the first to point out the in-plane special orthotropy of finite size graphene sheets, with Poisson's ratio values ν_{xy} and ν_{yx} equal to 0.43 and 0.52 respectively. The Authors have identified in-plane Poisson's ratios of 0.55 and 0.57 for uniaxially loaded SLGS with sliding conditions [1]. The higher in-plane Poisson's ratios recorded during the simulations of this paper can be explained by the significant Saint-Venant effects close to the clamped edge of the graphene sheet (Figure 1). The bonds belonging to the first 30 % of the long edges from the clamped side are all under compressive strains, as well as the vast majority of the vertical lengths of the graphene lattices (the dark blue lines of Figure 1). All the other C-C bonds are under tensile (positive strain), with the higher values close to the loaded and blocked atoms, and distributed in a bell-shape like surface between the clamped edge and the 20% of the SLGS length. Higher in-plane Poisson's ratio values have been proposed by Sakhaee-Pour and co-Authors [24] in SLGS truss assemblies where the equivalent properties of the C-C bonds have been calculated using the approach from Tserpes and Papanikos [25]. Those high PR values (1.129 – 1.141) can be explained by the high bending and shear deformation that the equivalent properties of the C-C bond induce [1].

3.2 Resonance

Table 2 shows the mechanical properties of the SLGS derived by the minimisation of the Hamiltonian corresponding to the first eigenmode of a fully clamped plate (Figure 2). The value of the (1, 1) natural frequency

Table 1
Mechanical Properties of Uniaxially Loaded SLGS

L_x [nm]	L_y [nm]	E_x [TPa]	ν_{xy}	d [nm]	L [nm]	ν	Y [TPa nm]	Force
7.6	2.09	4.13	0.71	0.055	0.135	– 0.78	0,227	AMBER
7.6	3.31	4.23	0.69	0.056	0.135	– 0.78	0.232	AMBER
7.6	6.55	4.38	0.65	0.055	0.135	– 0.78	0.241	AMBER
7.6	2.09	5.88	0.68	0.056	0.135	– 0.70	0.327	Morse
7.6	3.31	6.02	0.65	0.056	0.135	– 0.70	0.335	Morse
7.6	6.55	6.24	0.62	0.057	0.135	– 0.70	0.347	Morse

Table 2
Mechanical Properties Corresponding to the Minimisation of the Hamiltonian (Mode (1; 1))

L_x [nm]	L_y [nm]	E_x [TPa]	ν_{xy}	d [nm]	L [nm]	ν	Y [TPa nm]	$w_{1,1}$ [THz]	Force
8.16	7.33	6.91	-0.023	0.057	0.144	– 0.77	0.394	0.95	AMBER
8.16	3.55	6.82	-0.018	0.056	0.145	– 0.77	0.392	2.65	AMBER
8.16	1.81	6.91	-0.023	0.057	0.144	– 0.77	0.394	8.77	AMBER
8.16	7.33	8.61	0.039	0.055	0.144	– 0.71	0.465	1.07	Morse
8.16	3.55	8.45	0.045	0.057	0.145	– 0.71	0.481	3.01	Morse
8.16	1.81	8.44	0.046	0.057	0.144	– 0.71	0.481	10.04	Morse

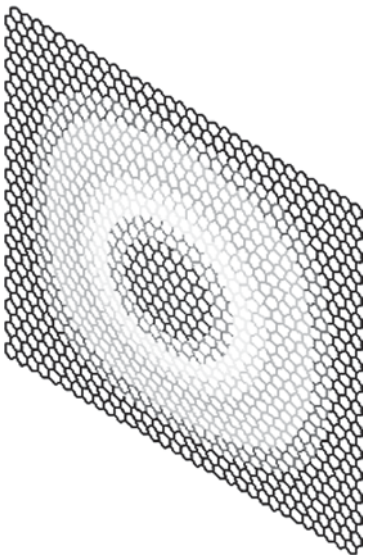

Figure 2: Mode (1, 1) for Fully Clamped SLGS (8.16 nm × 7.55 nm).

depends on the boundary conditions, dimensions and force model adopted. The linearised Morse potential provides the highest eigenvalues, with 1.07 THz for the 8.16 nm × 7.33 nm plate, while with the AMBER force model the resonance value is decreased by 11%. Sakhaee-Poor *et al*., [26] have calculated values on average 30% lower for fully clamped lattice structures SLGS with the C-C bonds modelled according to [25], and using the AMBER force model and a thickness of 0.34 nm. Like for the static case, the equivalent Poisson's ratio for the C-C bonds is significantly negative (– 0.77 and – 0.71 for the AMBER and Morse potentials respectively). The values of the plate thickness (between 0.056 and 0.057 nm) are close to the ones identified for the static case, equal to the values obtained from second generation Tersoff-Brenner potentials [18], close to the 0.062 nm of Brenner [6], and in line with the 0.052 nm of Duan and Wang [17]. The average bond length identified is however close to the upper bound of the values in open literature, between 0.144 and 0.145 nm. The low thickness and high equilibrium length values lead to a homogenised in-plane Poisson's ratio ν_{yx} close to zero, and marginally auxetic for the AMBER force model case, with NPR values up to – 0.023 for the largest clamped SLGS examined in this work. The homogenised Young's modulus calculated using [1] shows higher values compared to the ones calculated for the static tensile case, with an increase of 57% and 38% for the AMBER and Morse models respectively. For the dynamic case, the augmented equilibrium bond lengths induce a decrease of the bending stiffness of the bond itself, providing almost equivalent spring constants for the hinging and stretching in the AMBER model (6.84×10^{-7} N nm^{-1} and 6.52×10^{-7} N nm^{-1} respectively [1]). When the Morse potential is considered, the stretching spring constant is 20 % higher than the hinging one. The linear superposition in an hexagonal lattice of pure stretching lattice ($\nu \to -1$) and pure hinging ($\nu \to 1$) [27] with equal magnitudes leads to PR values for the graphene sheets close to zero, or even marginally auxetic considering the finite size and influence of the boundary conditions for the SLGS.

4. CONCLUSIONS

In this work we have shown some possible aspects of auxeticity in single layer graphene sheets, subjected to static loading and dynamic conditions (resonance). The auxeticity is revealed in the equivalent mechanical properties of the C-C bond, and therefore it is not an effective mechanical performance of the SLGS per se. However, when the minimisation of the Hamiltonian under resonance conditions corresponding to the first mode (fully clamped graphene sheet) is considered, the homogenised in-plane Poisson's ratio is close to zero, and becomes marginally auxetic when considering the simulations performed using the AMBER force model. In general, the thickness of the SLGS under minimised energy conditions is close to the values proposed in literature using Tersoff-Brenner and COMPASS potentials and force fields, while the tensile rigidities compare well with the ones in open literature, especially for the static loading case. This work shows also, for the first time, the effect that mechanical resonance conditions induce on the thickness value of the graphene.

REFERENCES

[1] F. Scarpa, S. Adhikari, and A. S. Phani, Effective Elastic Mechanical Properties of Single Layer Graphene Sheets, *Nanotechnology*, **20**, (2009), 065709.

[2] S. Stankovich, *et al.*, Graphene-Based Composite Materials, *Nature*, **442**, (2006), 202-206.

[3] J. Cho, J. J. Luo, and I M Daniel, Mechanical Characterization of Graphite/Epoxy Nanocomposites by Multi-Scale Analysis, *Comp. Sci. Tech.*, **67**, (2007), 2399.

[4] A. Hemmasizadeh, M. Mahzoon, and E. Hadi. A Method for Developing the Equivalent Continuum Model of a Single Layer Graphene Sheet, *Thin Solids Films*, **416**, (2008), 7636.

[5] P. P. Gillis, Calculating the Elastic Constants of Graphite, *Carbon*, **22**(4-5), (1984), 387.

[6] D. W. Brenner, Empirical Potential for Hydrocarbons for Use in Simulating the Chemical Vapor Deposition of Diamond Films, *Phys. Rev. B*, **42**(15), (1990), 9458-9471.

[7] C. D. Reddy, S. Rajendran, and K. M. Liew, Equilibrium Configuration and Elastic Properties of Finite Graphene, *Nanotechnology*, **17**, (2006), 864.

[8] I. W. Frank, D. M. Tanenbaum, A. M. van der Zande, and P. L. McEuen, Mechanical Properties of Suspended Graphene Sheets, *J. Vac. Sci. Technol. B*, **25**(6), (2007), 2558-2561.

[9] C. Lee, X. Wei, J. W. Kysar, and J. Hone, Measurement of the Elastic Properties and Intrinsic Strength of Monolayer Graphene, *Science*, **321**(5887), (2008), 385-388.

[10] O. A. Shenderova, V. V. Zhirnov, and D. W. Brenner, Carbon Materials and Nanostructures, *Crit. Rev. Solid State Mater. Sci.*, **27**, (2002), 227.

[11] H. Goldstein, C. P. Poole, and J. L. Safko, *Classical Mechanics*, Addison-Wesley, Cambridge, MA, (1950).

[12] W. D. Cornell, *et al*., *A Second. J. Am. Chem. Soc.*, 117 (A Second Generation Force Field for the Simulation of Proteins, Nucleic Acids, and Organic Molecules), (1995), 5179.

[13] T. Belytschko, S. P. Xiao, and R. S. Ruoff, Atomistic Simulations for Nanotube Fracture, *Phys. Rev. B*, **65**, (2002), 235430.

[14] T. K. Aneko, On Timoshenko's Correction for Shear in Vibrating Beams, *J. Phys. D: App. Phys.*, **8**, (1974), 1927.

[15] M. I. Friswell, and J. E. Mottershead, Finite Element Model Updating in Structural Dynamics, Kluwer Academic Publishers, (1995).

[16] C. Seoanez, F. Guinea, and A. H. Castro Neto, Dissipation in Graphene and Nanotube Resonators, *Phys. Rev. B*, **76**, (2007), 125427.

[17] W. H. Duan, and C. M. Wang, Nonlinear Bending and Stretching of a Circular Graphene Sheet Under a Central Point Load, *Nanotechnology*, **20**, (2009), 075702.

[18] Y. Huang, J. Wu, and K. C. Hwang, Thickness of Graphene and Single wall Carbon Nanotubes, *Phys. Rev. B*, **74**, (2006), 245413.

[19] D. Caillerie, A. Mourat, and A. Raoult, Discrete Homogenization in Graphene Sheet Modeling, *J. Elasticity*, **84**, (2006), 33.

[20] Z. Tu, and Z. Ou-Yang, Single-Walled and Multi-Walled Carbon Nanotubes Viewed as Elastic Tubes with the Effective Young's Moduli Dependent on Layer Number, *Phys. Rev. B*, **65**, (2002), 233407.

[21] K. N. Kudin, G. E. Scuseria, and B. I. Yakobson, C2F, BN and C Nanoshell Elasticity from ab Initio Computations, *Phys. Rev. B*, **64**, (2001), 235406.

[22] O. L. Blakslee, *et al*., Elastic Constants of Compression-Annealed Pyrolitic Graphite, *J. App. Phys.*, **44**(8), (1970), 3373.

[23] T. Chang, and H. Gao, Size-Dependent Elastic Properties of a Single Walled Carbon Nanotube via a Molecular Mechanics Model, *J. Mech. Phys. Solids*, **51**, (2003), 1059.

[24] A. Sakhaee-Pour, M. T. Ahmadian, and A. Vafai, Potential Application of Single-Layered Graphene Sheet as Strain Sensor, *Solid State Comm.*, **147**(7-8), (2008), 336-340.

[25] K. I. Tserpes, and P. Papanikos, Finite Element Modelling of Single-Walled Carbon Nanotubes, *Comp. B*, **36**, (2005), 468.

[26] A. Sakhaee-Pour, M. T. Ahmadian, and R. Naghdabadi, Vibrational Analysis of Single-Layered Graphene Sheets, *Nanotechnology*, **19**, (2008), 085702.

[27] I. G. Masters, and K. E. Evans, Models for the Elastic Deformation of Honeycombs, *Comp. Struct.*, **35**, (1996), 403-422.